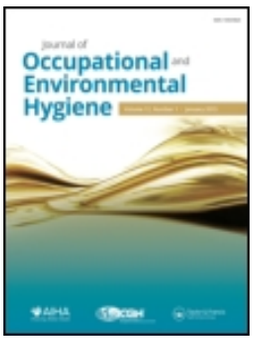

Taylor & Francis
Taylor & Francis Group

Journal of Occupational and Environmental Hygiene

ISSN: 1545-9624 (Print) 1545-9632 (Online) Journal homepage: http://www.tandfonline.com/loi/uoeh20

Deposition of graphene nanomaterial aerosols in human upper airways

Wei-Chung Su, Bon Ki Ku, Pramod Kulkarni & Yung Sung Cheng

To cite this article: Wei-Chung Su, Bon Ki Ku, Pramod Kulkarni & Yung Sung Cheng (2016) Deposition of graphene nanomaterial aerosols in human upper airways, Journal of Occupational and Environmental Hygiene, 13:1, 48-59, DOI: 10.1080/15459624.2015.1076162

To link to this article: http://dx.doi.org/10.1080/15459624.2015.1076162

Accepted author version posted online: 28 Aug 2015.
Published online: 06 Jan 2016.

JOURNAL OF OCCUPATIONAL AND ENVIRONMENTAL HYGIENE
2016, VOL. 13, NO. 1, 48–59
http://dx.doi.org/10.1080/15459624.2015.1076162

Taylor & Francis
Taylor & Francis Group

Deposition of graphene nanomaterial aerosols in human upper airways

Wei-Chung Su[a], Bon Ki Ku[b], Pramod Kulkarni[b], and Yung Sung Cheng[a]

[a]Lovelace Respiratory Research Institute, Albuquerque, New Mexico; [b]National Institute for Occupational Safety and Health, Cincinnati, Ohio

ABSTRACT

Graphene nanomaterials have attracted wide attention in recent years on their application to state-of-the-art technology due to their outstanding physical properties. On the other hand, the nanotoxicity of graphene materials also has rapidly become a serious concern especially in occupational health. Graphene naomaterials inevitably could become airborne in the workplace during manufacturing processes. The inhalation and subsequent deposition of graphene nanomaterial aerosols in the human respiratory tract could potentially result in adverse health effects to exposed workers. Therefore, investigating the deposition of graphene nanomaterial aerosols in the human airways is an indispensable component of an integral approach to graphene occupational health. For this reason, this study carried out a series of airway replica deposition experiments to obtain original experimental data for graphene aerosol airway deposition. In this study, graphene aerosols were generated, size classified, and delivered into human airway replicas (nasal and oral-to-lung airways). The deposition fraction and deposition efficiency of graphene aerosol in the airway replicas were obtained by a novel experimental approach. The experimental results acquired showed that the fractional deposition of graphene aerosols in airway sections studied were all less than 4%, and the deposition efficiency in each airway section was generally lower than 0.03. These results indicate that the majority of the graphene nanomaterial aerosols inhaled into the human respiratory tract could easily penetrate through the head airways as well as the upper part of the tracheobronchial airways and then transit down to the lower lung airways, where undesired biological responses might be induced.

KEYWORDS
Aerosol; deposition efficiency; graphene nanomaterial; human airway

Introduction

Graphene is a one-atom-thick, platelet-like nanomaterial constructed by pure carbon atoms first produced only a decade ago,[1] whereas it has drawn substantial scientific attention and technology interest today. The distinctive physical characteristics of the graphene nanomaterial in terms of mechanical strength, physical elasticity, thermal conductivity, and electrical property have made graphene a unique material for application in various high-tech products in areas of electronics, energy storage, and composite materials.[2] Besides, graphene nanomaterials also have proven to possess a great potential for biomedical and biotechnology application such as drug delivery, biosensing, and tissue engineering.[3] Because of these potential and valuable applications, the graphene nanomaterial has become one of the intensively studied nanomaterials both in industry and academia.[4,5]

Despite its promising future, the nanotoxicity of the graphene nanomaterials has also rapidly become a serious concern. According to published toxicity studies on graphene nanomaterials (including graphene nanosheets, few-layer graphene, graphene oxide, etc.),[6] mice administrated with graphene nanomaterials could induce lung granuloma formation,[7] inflammation cell infiltration, pulmonary edema,[8] severe and persistent lung injury,[9] and acute pulmonary inflammatory and frustrated alveolar phagocytosis.[10] Some *in vitro* cell culture studies also indicated that graphene nanomaterials could induce cytotoxic effects in human neuronal cells,[11] cause viability decreasing and apoptosis in human lung cells,[12] and show cell sensitivity and concentration-dependent cytotoxicity in alveolar basal epithelial cells.[13] Based on these research results, it would be safe to assume that the inhalation and deposition of graphene nanomaterial aerosols in the human respiratory tract might also induce potential adverse biological responses.

Due to the fact that graphene nanomaterials inevitably could become airborne during product harvesting, handling, and reactor cleaning processes in graphene manufacturing workplaces,[14] workers and researchers in

CONTACT Wei-Chung Su wsu@LRRI.org Lovelace Respiratory Research Institute, 2425 Ridgecrest Dr. SE, Albuquerque, NM 87108.
Color versions of one or more of the figures in the article can be found online at www.tandfonline.com/uoeh.

graphene associated manufactories and laboratories could involuntarily inhale graphene nanomaterial aerosols. The consequent deposition of graphene nanomaterial aerosols in the worker's respiratory tract could therefore pose possible adverse health effects. Thus, the risk of worker exposure to graphene aerosols in related workplaces should be considered an essential occupational health issue in today's nanotechnology era. The investigation of the graphene aerosol airway deposition, hence, should be the indispensable component of an integral graphene occupational health study.

However, because the dimension of the graphene nanomaterial aerosol is extremely small, it is infeasible to apply conventional airway deposition methods on graphene aerosols for conducting airway replica deposition studies. The conventional methods for aerosol airway replica deposition study involve either radioactive or fluorescent labeled test aerosols.[15–17] These experimental methods are considered technically difficult to apply on graphene aerosols not only because of the required radioactive facilities, but also due to the measurement limitation for radioactive and fluorescent tagged nanomaterial aerosols. Therefore, there is a need of finding an alternative experimental method to carry out airway replica deposition experiments using nanomaterial aerosols. For this reason, a novel experimental approach has been developed in our laboratory and employed previously in our laboratory for two airway replica deposition studies.[18,19] A great number of quality airway deposition data were acquired by using this experimental approach. In this study, this novel approach was employed again and applied on graphene nanomaterial aerosols to obtain original airway deposition data, and it is also the first time in the literature that graphene aerosol was used in airway replica deposition experiments. The experimental data obtained is believed to be valuable for assessing the risk of worker exposure to airborne graphene nanomaterials in related occupational settings, since the deposition data obtained from the upper airways in this study can be utilized to estimate the portion of the inhaled graphene aerosols entering the lower airways. In addition, the deposition data acquired from this study can also be used to validate mathematical models newly developed for predicting the airway dosimetry of nanomaterial aerosols.

Method

The experimental approach, briefly speaking, is to generate size classified graphene nanomaterial aerosols based on preselected diameters and then deliver them into the human airway replica. In the deposition study, the graphene aerosol concentration in each airway section is the primary data to measure. By obtaining associated concentration ratios for all airway sections on the airway replica, the graphene airway deposition efficiency and fractional deposition map can then be calculated. The following procedures illustrate the details of the experimental approach for the deposition study.

Graphene nanomaterial aerosolization

The graphene nanomaterial used for generating graphene aerosols in this study was purchased from Cheap Tube Inc. (Brattleboro, VT, USA). This graphene nanomaterial was in grade 3, which contained 97% purity, 2 μm in platelet diameter, and 600–750 m^2/g surface area. Figure 1a shows the morphology of the graphene bulk material under a transmission electron microscope (TEM). As can be seen, the graphene nanomaterial was severely agglomerated. Graphene in crumpled, crushed, and platelet-like shapes were found in the bulk material. To aerosolize the graphene nanomaterial for the deposition study, an electrospray (Model 3480, TSI Inc., Shoreview, MN, USA) was employed. The electrospray is a widely applied aerosolization device capable of generating airborne nanomaterials with uniform size and shape. The electrospray has been used in a variety of studies for generating nanoparticles, including carbon nanotubes and engineered nanomaterials.[20,21] To use electrospray for generating graphene aerosols, graphene suspension was prepared by adding 90 mg graphene nanomaterial into 20 ml ethanol alcohol with 5 μl ammonium acetate as a buffer solution. The graphene suspension was treated with ultrasonicator for 10 minutes each time before being added into the electrospray for generating graphene aerosols. The capillary used for transporting graphene suspension in the electrospray was made of silica with ID of 100 μm and OD of 360 μm (Polymicro Technologies, Phoenix, AZ). When operating the electrospray, 4.0 psi differential pressure was set on the electrospray to push graphene suspension from the sample vial through the capillary tube to the opening end of the capillary. A high voltage of 2.3 kV was added to the capillary, which generated an electrical field at the end of the capillary and pulled the graphene suspension from the capillary to form tiny droplets. A mix of filtered air and CO_2 (0.1 L/min each) was then used to evaporate ethanol in the droplets to have only graphene aerosols remaining in the air. Before leaving the outlet of the electrospray, the graphene aerosols were neutralized by a Po-210 ionizer.

Graphene nanomaterial aerosol characterization

The graphene aerosols were then delivered into a differential mobility analyzer (DMA, Model 3071A, TSI Inc., Shoreview, MN) for size classification. The principle of

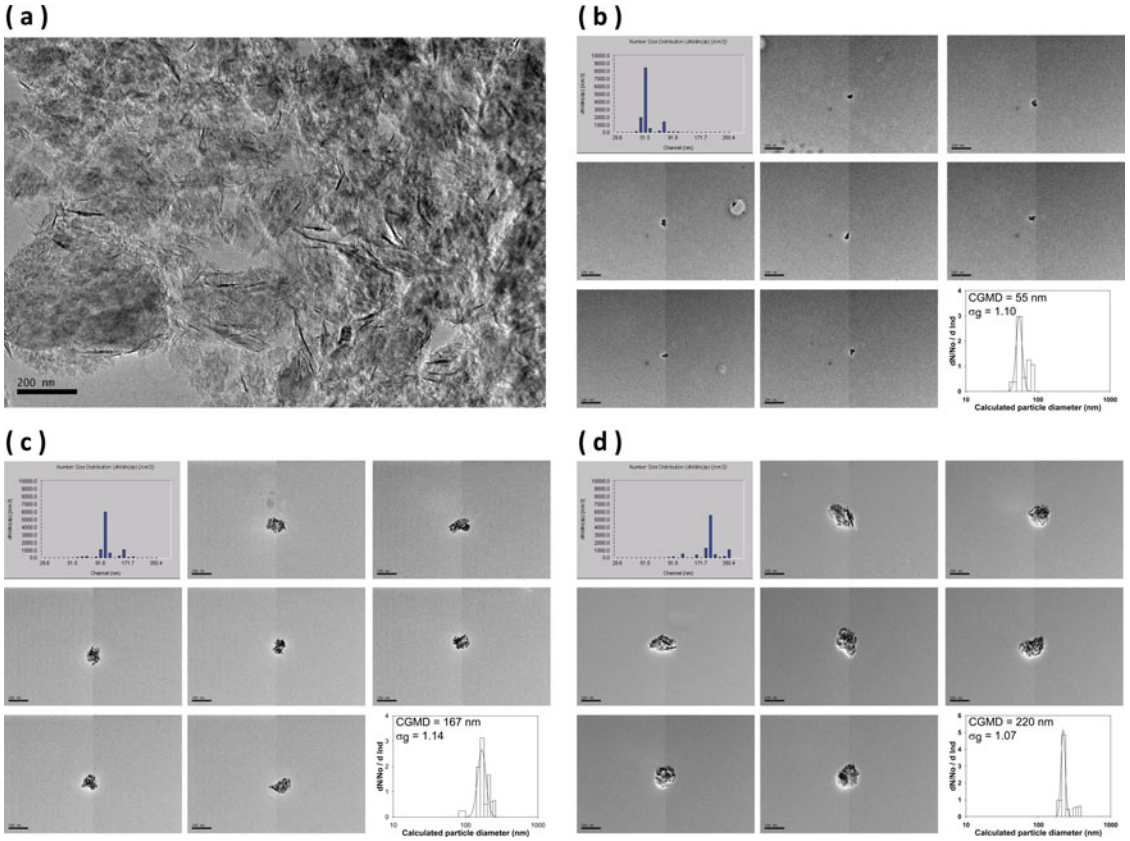

Figure 1. The morphology of graphene bulk material and the size classified graphene nanomaterial aerosols (a) bulk materual, (b) 51 nm, (c) 101 nm, and (d) 215 nm. (Also shown are measured size distribution, and calculated area equivalent diameter. CGMD = count geometric median diameter; σ_g = geometric standard deviation; reference bars in each subgraphe from (b) to (d) represent 200 nm).

the DMA is to use the balance between the electrostatic force and the air drag force acting on aerosols to size classify them from polydisperse aerosols to monodisperse aerosols according to the electrical mobility diameter (d_B) of the aerosol. To size classify graphene aerosols, graphene aerosols of 1 L/min were delivered into the DMA, and the DMA was set with parameters (sheath flow of 10 L/min and suitable voltages) based on target/designated classification diameters (d_B). The designated classification diameters for this deposition study were 51, 101, and 215 nm. In order to ascertain the size classified graphene aerosols leaving the DAM possessing the designated classification diameter, a sequential mobility particle sizer (SMPS, GRIMM Aerosol Technik GmbH & Co., Germany) was connected to the output of the DAM to monitor the size distribution of the classified graphene aerosols. Samples of the size classified graphene aerosols were also collected on TEM grids with a point-to-plane electrostatic precipitator (In-Tox Products, Albuquerque, NM) for needed morphology analysis. The graphene aerosol morphology analysis was conducted by a JEOL 2010 TEM (JEOL Ltd., Tokyo, Japan). Pictures of graphene aerosol were taken for each designated classification diameter when inspected by the TEM. Figures 1b–d show some characteristics of the size classified graphene aerosols: the aerosol morphology, size distribution (measured by the SMPS), and associated area equivalent diameter (calculated from the particle envelop area measured by corresponding TEM pictures).

To further study the aerodynamic diameter (d_{ae}) of the size classified graphene aerosols, an aerosol particle mass analyzer (APM, Kanomax USA, Inc., Andover, NJ) was used for this purpose. The principle of the APM is to utilize the balance between the electrostatic force and centrifugal force acting on the test aerosols to acquire the mass information of the test aerosols. By using the APM together with the DMA to form a DMA-APM tandem setup, and following the experimental procedure published in literature,[22,23] the aerodynamic diameter of the size classified graphene aerosols can then be estimated.

Human airway replicas

In this study, the deposition experiments were conducted in two airway replicas: nasal airway and oral-to-lung airway. For the nasal deposition study, a nasal airway replica constructed by 77 acrylic plates (1.5 mm in thickness

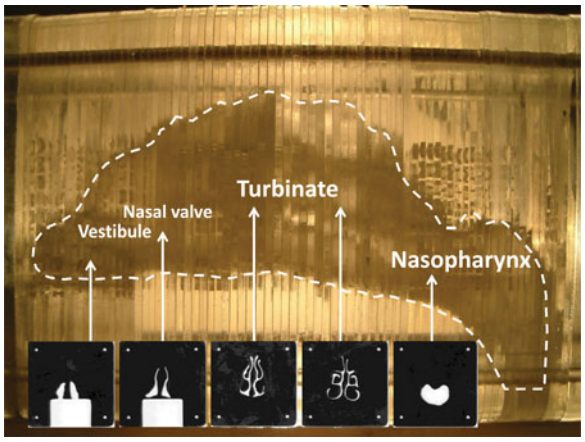

Figure 2. The schematic of the human nasal airway replica.

for each plate) was used. This nasal airway replica was made based on a set of *in vivo* head MRI scans of a male adult. This nasal airway replica consists of detailed nasal airway structures from the nostril, vestibule, nasal valve, and turbinate to the nasopharynx. The airway geometry and the air flow field in this nasal airway replica have already been well studied,[24,25] and this nasal airway replica has been employed in our laboratory for a number of airway deposition studies using spherical particles, fiber aerosols, and carbon nanotubes.[18,26,27] Deposition results obtained from this nasal airway replica have successfully demonstrated this replica is able to provide reliable experimental data for aerosol nasal airway deposition study. Figure 2 shows the nasal airway replica used in this study with individual acrylic plates selected from some major airway sections. For the oral-to-lung airway deposition study, a human respiratory tract replica made of conductive silicone rubber (KE-4576, Shin-Etsu Chemical Co., Ltd., Tokyo, Japan) was used. The original production mold of this human respiratory tract replica was made from a cadaver.[28] This human oral-to-lung airway replica consists of an oral cavity, pharynx, larynx, and tracheobronchial airways down to part of the 4th lung generation. The geometry and dimension of this oral-to-lung airway replica also has been well studied previously.[29] This oral-to-lung airway replica has been frequently used in our laboratory for aerosol airway deposition studies and numerous representative experimental data were acquired.[17,19,30,31] Figure 3 shows the physical model of the oral-to-lung airway replica in conjunction with the illustration of the airway structure. In this study, due to the experimental approach designed for the airway deposition study, several identical oral-to-lung airway replicas were trimmed based on the human airway structure to have only certain lung generations remain on the replica. The trimmed airway replicas made for this study are all demonstrated in Figure 3.

Estimation of graphene aerosol airway deposition

Figure 4a shows the experimental setups of the graphene aerosol airway deposition study using the nasal airway and the oral-to-lung airway, respectively. As can be seen, the DMA size classified graphene aerosols were delivered straight into the human airway replica for deposition experiments. The SMPS was employed again in the experiment for measuring the average concentration of the graphene aerosol in the airway replica. When measuring the average concentration, the SMPS output channels were rearranged to have only one channel that matches the designated classification diameter to show on the SMPS monitor (the channel showing the peak concentration in SMPS subgraphs in Figures 1b–d). In this way, it permitted the tracking of the concentration variation of the size classified graphene aerosol over a period of time. The graphene aerosol average concentration (C) was measured in a pair (C_{inlet}, C_{outlet}) at both the inlet and outlet of the airway replica by using a three way valve as shown in Figures 4a and 4b. For the nasal airway replica, since there is only one inlet and one outlet (nasopharynx) on the entire replica, only one pair of the graphene aerosol average concentration was required to determine the airway deposition. However, for the oral-to-lung airway replica, there is more than one outlet in the airway replica. Therefore, several pairs of average concentration were needed to determine the graphene deposition in different airway sections. When all of the required concentration pairs were obtained, a set of corresponding concentration ratios, C_{outlet}/C_{inlet}, could then be calculated. These concentration ratios were the primary data as well as the foundation in this study to estimate the deposition fraction of graphene aerosol in the human airways. The deposition fraction in this study is defined as the percentage (%) of the graphene aerosols deposited within a certain airway section to the total graphene aerosols that entered the entire airway replica (the entire nasal or oral-to-lung airway replica).

In the nasal airway deposition study, inspiratory flow rates of 15, 30, and 43.5 L/min were used in the experiment. These flow rates represent the inhalation flow rates of a worker from being at an at-ease status to having moderate workloads.[32] The C_{outlet}/C_{inlet} concentration ratios obtained from SMPS measurement can be directly used to calculate the nasal deposition fraction, D_{nasal}:

$$D_{nasal}(\%) = \left(1 - \frac{C_{outlet}}{C_{inlet}}\right) \times 100. \quad (1)$$

In the oral-to-lung airway deposition experiments, an inspiratory flow rate of 43.5 L/min was used for the deposition study. The flow rate distribution in the oral-to-lung airway for this inspiratory flow rate has already been well

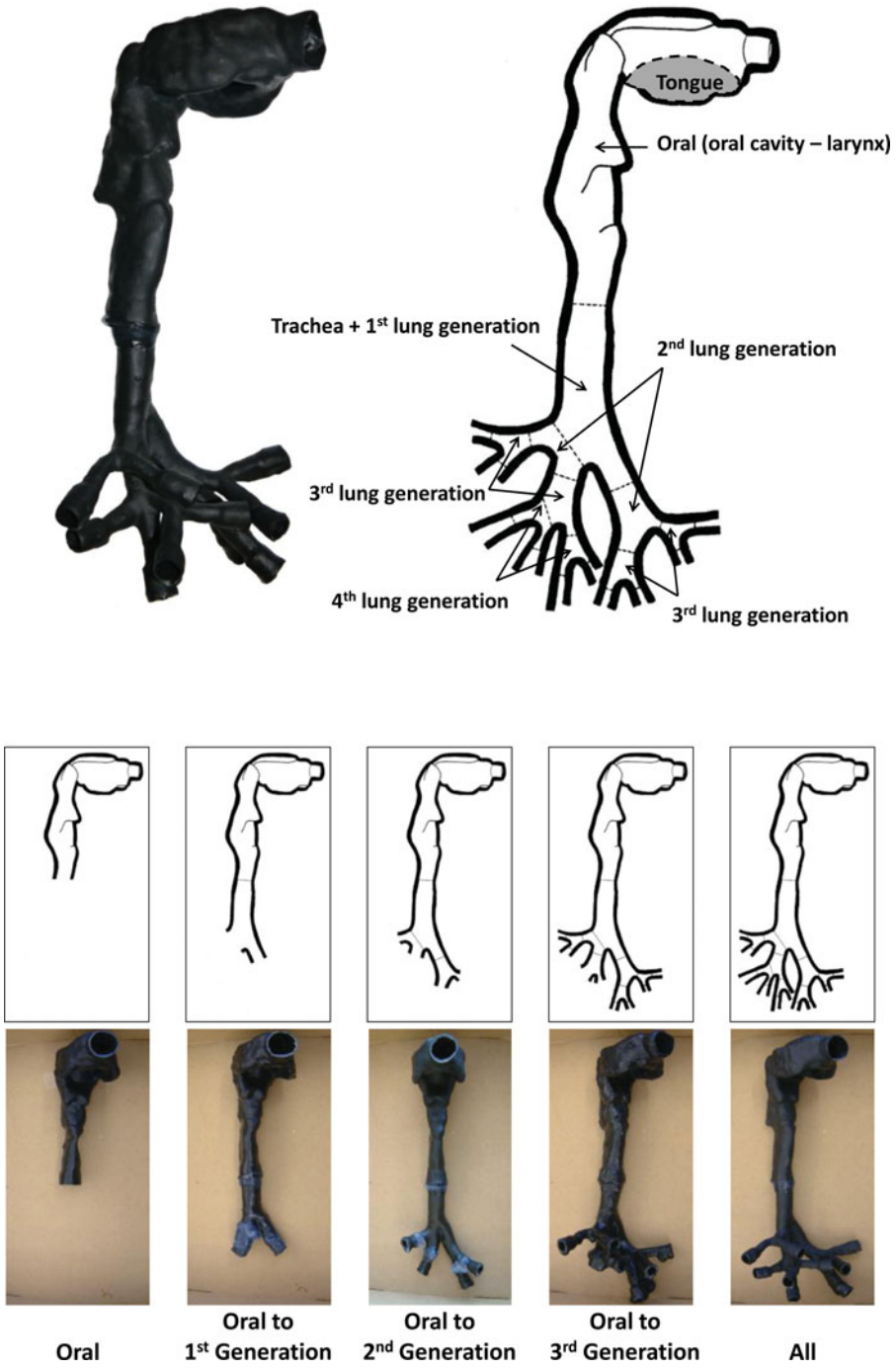

Figure 3. The schematic of the human oral-to-lung airway replica and the trimmed replicas.

defined elsewhere.[33] To estimate the oral airway deposition fraction, the experimental procedure is similar to that done in the nasal airway study since the oral airway has only one inlet and one outlet as the nasal airway. However, to estimate the deposition fraction for lung bifurcations in the tracheobronchial airways of the oral-to-lung airway replica, it is relatively much more difficult and complicated and is depicted in detail as follows: given a typical lung bifurcation has one parent tube (p) and two daughter tubes (d_1 for the left daughter tube and d_2 for the right daughter tube), the graphene aerosol deposition fraction in that lung bifurcation can be calculated by the equation below derived from the principle of mass conservation:[19]

$$D_{lung}(\%) = \left(\frac{Q_p}{Q_{oral}} \frac{C_p}{C_{oral}} - \frac{Q_{d1}}{Q_{oral}} \frac{C_{d1}}{C_{oral}} - \frac{Q_{d2}}{Q_{oral}} \frac{C_{d2}}{C_{oral}} \right) \times 100, \quad (2)$$

where D_{lung} is the deposition fraction (in percentage) of graphene aerosol in a certain lung bifurcation; Q_p/Q_{oral},

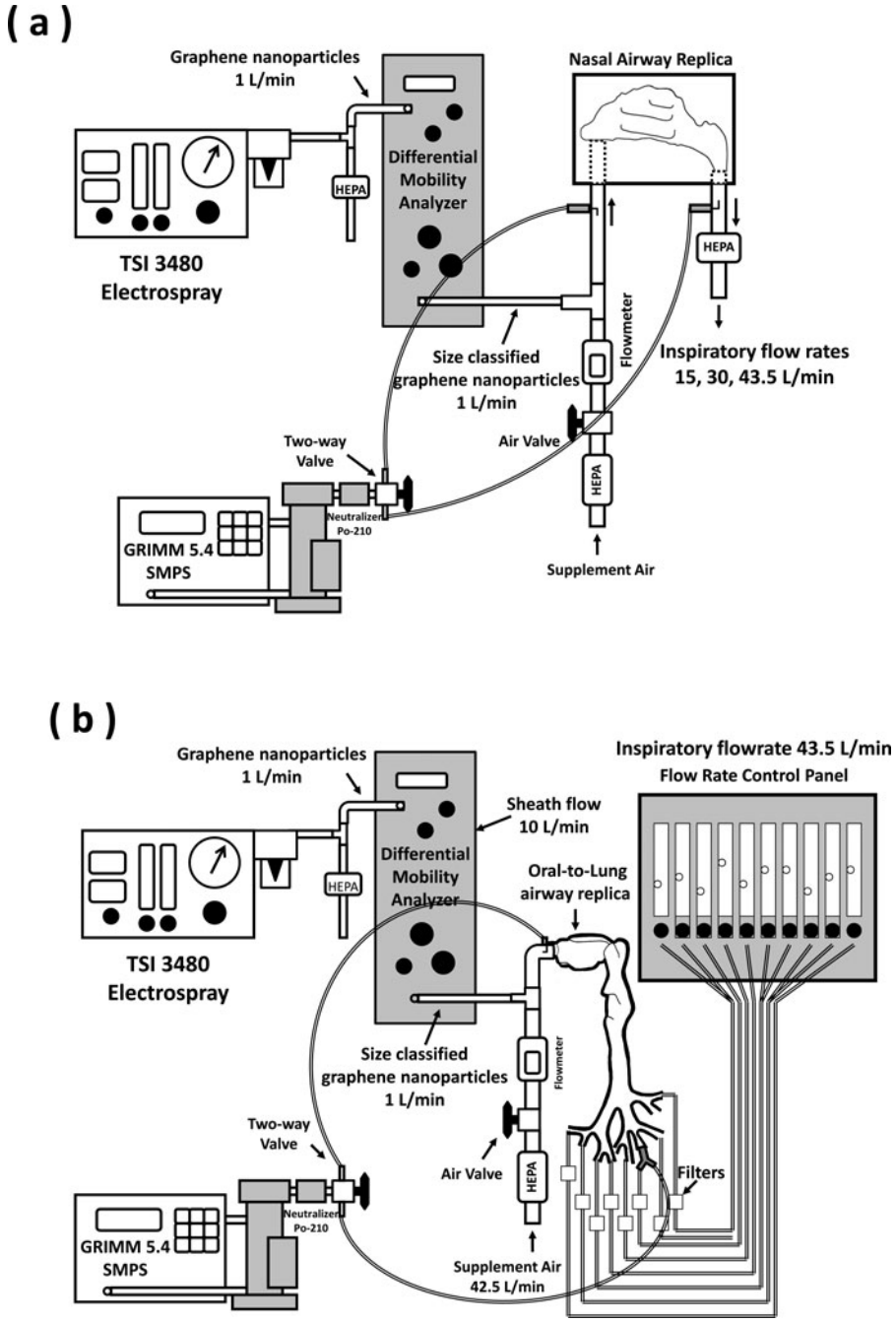

Figure 4. The experimental setup of graphene aerosol deposition study in (a) nasal airway and (b) oral-to-lung airway.

Q_{d1}/Q_{oral}, and Q_{d2}/Q_{oral} are respective flow rate ratios of the flow rate in the parent tube, left daughter tube, and right daughter tube in regard to the total flow rate entering the oral airway (43.5 L/min in this study); C_p/C_{oral}, C_{d1}/C_{oral}, and C_{d2}/C_{oral}, are the graphene aerosol average concentration ratios measured at the parent tube, left daughter tube, and right daughter tube, respectively (the C_{outlet}/C_{inlet} mentioned above). Here, since the total flow rate and the flow rate distribution in the entire oral-to-lung airway replica (including the tracheobronchial airways) are already defined, the Q_p/Q_{oral}, Q_{d1}/Q_{oral}, and Q_{d2}/Q_{oral} in Equation (2) therefore are all known variables. Thus, to calculate the deposition fraction for a lung bifurcation by using Equation (2), the only unknowns in Equation (2) are those concentration ratios. Once the concentration ratios are measured for all the lung bifurcations on the oral-to-lung airway replica, the graphene aerosol deposition fraction in each lung bifurcation can be estimated, and a complete airway fractional deposition map can then be constructed. To facilitate measuring all necessary C_{outlet}/C_{inlet} concentration ratios in the oral-to-lung airway replica, trimmed airway replicas shown in

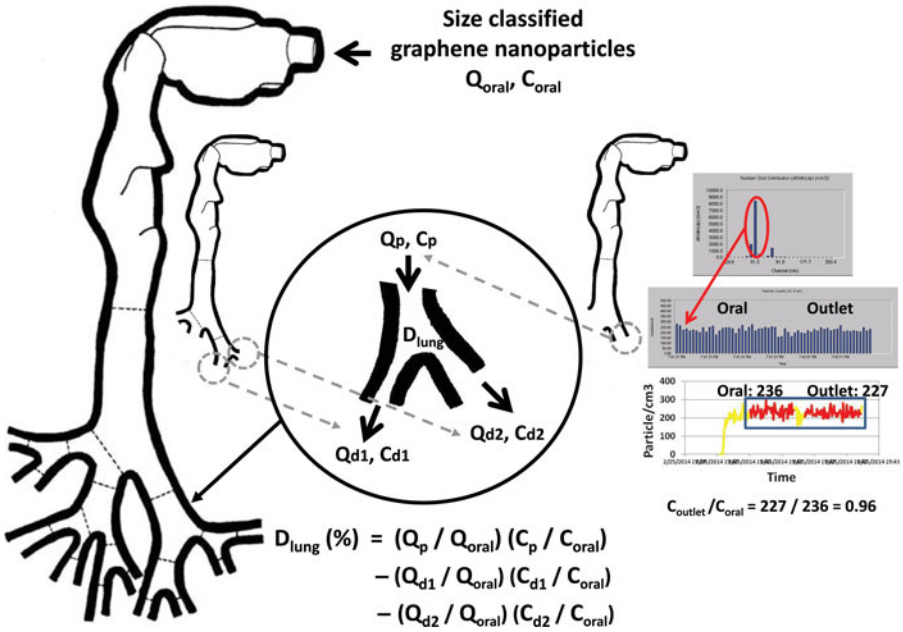

Figure 5. The procedure to obtain the graphene aerosol average concentration ratio for a lung bifurcation, and the calculation for the associated deposition fraction.

Figure 3 were made for this purpose. With these trimmed airway replicas, C_{outlet}/C_{inlet} concentration ratio for each lung tube on the oral-to-lung airway replica can be measured. Figure 5 summarizes the procedure of how to obtain the C_{outlet}/C_{inlet} for a certain lung bifurcation in the oral-to-lung airway replica together with the calculation to estimate the deposition fraction for that lung bifurcation.

In this study, for every experimental condition (i.e., combination of different lung tube flow rates and graphene classification diameters), the C_{inlet} and C_{outlet} were measured for at least 70 sec individually to obtain ideal C_{outlet} and C_{inlet} averages, and each experimental condition was repeated a minimum of three times for obtaining statistically meaningful results. When preparing the nasal airway or the oral-to-lung airway replica for the deposition experiment, a thin layer of silicon oil (550 Fluid, Dow Corning Co., Midland, MI) was applied onto the inside surface of the airway replica (accompanying with overnight dripping) to simulate the wet surface nature of the real human airways. Also, in this study, separate experiments were carried out by using size classified NaCl aerosols with the same designated classification diameters as the graphene aerosols for investigating the particle delivery efficiency of the experimental setup. From the investigation conducted, a set of delivery efficiency correction factors (F) were acquired covering all experimental conditions and airway replicas in this study. These delivery efficiency correction factors, F, considered the graphene aerosol delivery loss due to diffusion while the aerosols are transporting in the tubing system of the experimental setup. The F acquired was then incorporated into Equations (1) and (2) to calculate the final airway deposition fraction: *True concentration ratio* $= F \times$ *Measured concentration ratio*. In this way, it is believed that a more accurate aerosol airway deposition calculation can be achieved given that the system particle diffusion loss has been well addressed. For the sake of brevity, the experimental procedure and results regarding the investigation of the particle delivery efficiency correction factors are not repeated here; all of the details can be found in our previous works.[18,19]

Results

Figure 6 shows the calculated aerodynamic diameter (d_{ae}) and effective density (ρ_{eff}) of the size classified graphene aerosol acquired from the DMA-APM tandem study. Figures 7 and 8 display the fractional deposition map of size classified graphene aerosols in the human nasal and oral-to-lung airways, respectively. Figure 9 presents the deposition efficiency of the graphene aerosol in the nasal (Figure 9a) and oral (Figure 9b) airways as a function of particle impaction parameter $d_{ae}{}^2Q$ (Q is the flow rate in the airway). The particle impaction parameter is a common physical parameter used for presenting aerosol airway deposition data in irregular or complicated human airways such as nasal and oral airways, and the deposition efficiency is defined as the ratio of the aerosol amount deposited within a specific airway section to the total aerosol amount entering that specific airway section. In this study, the graphene aerosol amount

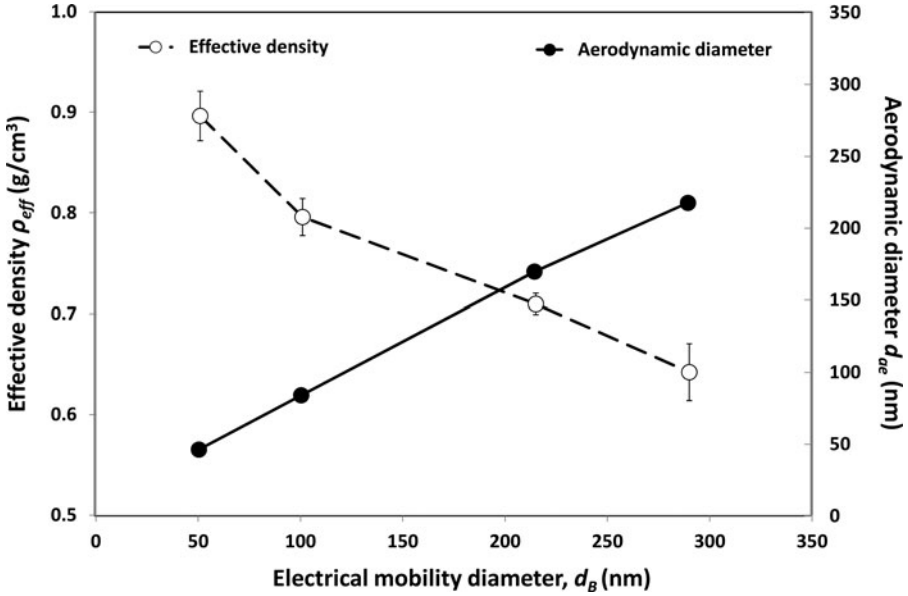

Figure 6. The effective density and the aerodynamic diameter of the size classified graphene aerosols as a function of the classification diameter (electrical mobility diameter).

that entered an airway section, as well as the aerosol amount deposited within the airway section, can be back-calculated by the data shown in the fractional deposition maps in Figures 7 and 8. Also shown in Figure 9a are some published nasal deposition data acquired by using spherical particles.[27,34,35] Similarly, together presented in Figure 9b are published oral deposition data using spherical particles.[30] Figures 10a–c show the deposition efficiency in the tracheobronchial airways from the 1st to the 3rd lung generation. The deposition efficiencies were plotted against the Stokes number. The Stokes number for a particle in a lung bifurcation is expressed as $Stk = \rho_o\, d_{ae}\, U_s$ / $18\eta D$ (ρ_o is the density of water, d_{ae} is displayed in Figure 6, U_s is the mean air velocity in the parent tube, η is the air viscosity, and D is the mean diameter of the parent tube). The Stk is a dimensionless physical parameter frequently used for presenting aerosol deposition in lung

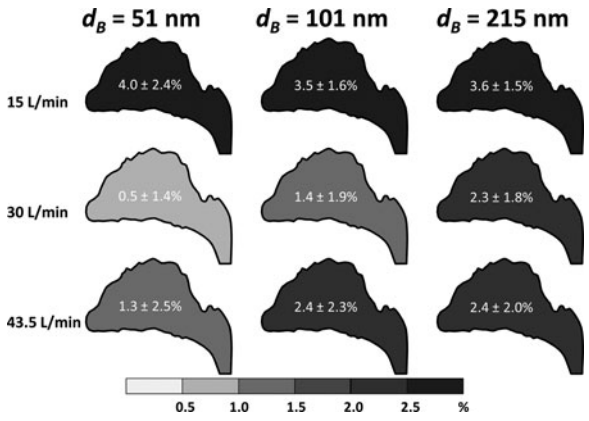

Figure 7. The deposition fraction of graphene aerosols in the human nasal airway.

bifurcations. Also shown in Figure 10 are deposition data obtained from separate experiments using size classified NaCl aerosols in this study, as well as other spherical particle data acquired previously from our laboratory.[17] (All of the non-graphene data shown in Figures 9 and 10 are for the purpose of data comparison, since the test particles are all isometric, and were all obtained from the same nasal and oral-to-lung airway replicas.)

Discussion

As can be seen in Figure 1, the graphene aerosols could be ideally size classified by their d_B. For each designated classification diameter (51, 101, or 215 nm), an apparent peak concentration was shown on the SMPS right at the channel bar corresponding to the designated classification diameter. This result implies that the majority of the graphene aerosols coming out of the DMA possessed the same d_B, which can also be evidently seen by the morphology of the graphene aerosols shown on Figure 1. Based on this, it is warranted that airway deposition data obtained in this study under a certain designated classification diameter were all generated by graphene aerosols with a same physical property, d_B.

Also, from the graphene aerosol morphology presented in Figure 1, it is noticeable that the graphene aerosols were generally isometric in shape. The increase of the classification size only made the particle diameter increase but remained the particle morphology basically unchanged. When taking a close look at the morphology of the graphene aerosol, it was found that the graphene aerosols were all constructed by agglomerated

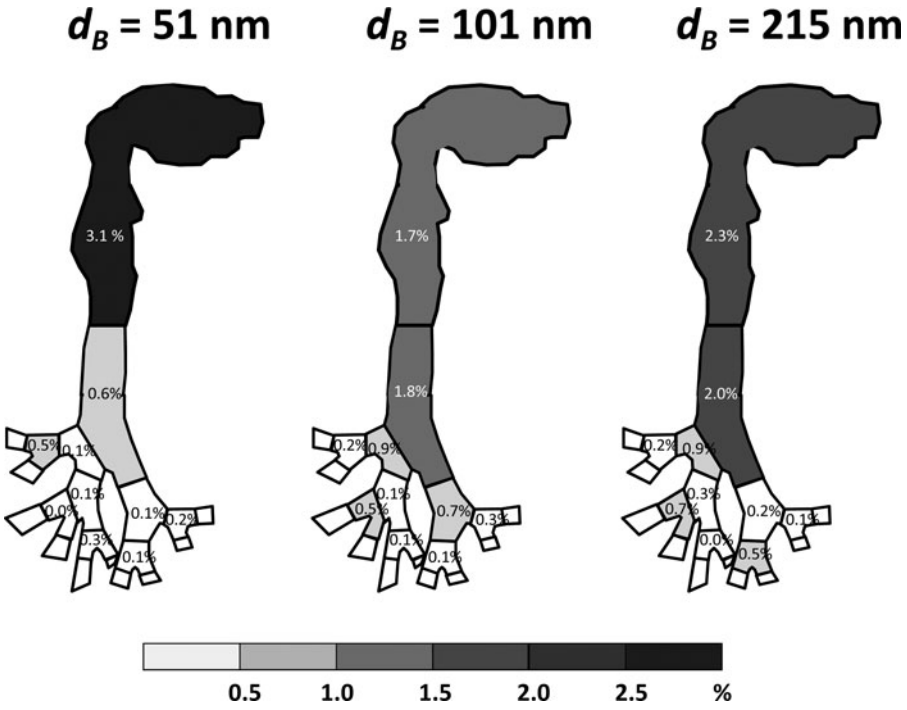

Figure 8. Fractional deposition maps of graphene aerosols in the human respiratory tract replica (data uncertainty were 0.4–3.4%, 0.3–3.6%, and 0.4–2.4% for d_B = 51 nm, 101 nm, and 215 nm, respectively).

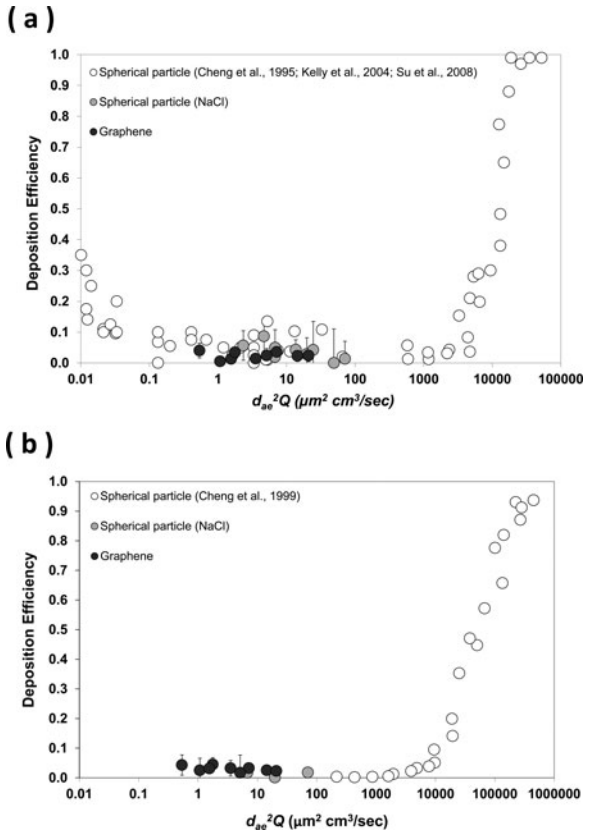

Figure 9. The deposition efficiency of graphene aerosols in (a) nasal airway and (b) oral airway as a function of the particle impaction parameter.

graphene platelets. This might be due to the fact that all of the graphene aerosols were formed by evaporated graphene suspension droplets. The evaporation of the alcohol portion in a graphene suspension droplet resulted in droplet shrinking and graphene nanoplatelet agglomerating, which eventually formed the graphene aerosol morphology presented. A published field sampling study conducted at a graphene manufactory also indicated that graphene aerosols released in the workplaces was primarily graphene agglomerates.[14] Therefore, in this study, the use of size classified graphene aerosols in the form of agglomeration for airway deposition experiments is considered realistic and also practical to a certain extent. It is widely accepted that graphene agglomerates, once deposit in the lung airways, will gradually disperse in the lung mucus where the nanotoxicity effects of the graphene platelets found in those *in vivo* and *in vitro* studies can then be seen.

Figure 6 indicates that the acquired effective density, ρ_{eff}, of the size classified graphene aerosols were generally less than 1 g/cm^3 (the density of carbon: ~2.0 g/cm^3), and the ρ_{eff} decreased as the classification diameter increased. This result implies that the agglomerated graphene aerosols generated in this study contain a considerable portion of empty space within them (loose structure), and the larger the particle size, the larger the portion of the empty space. This phenomenon is in agreement with what was found in other published research

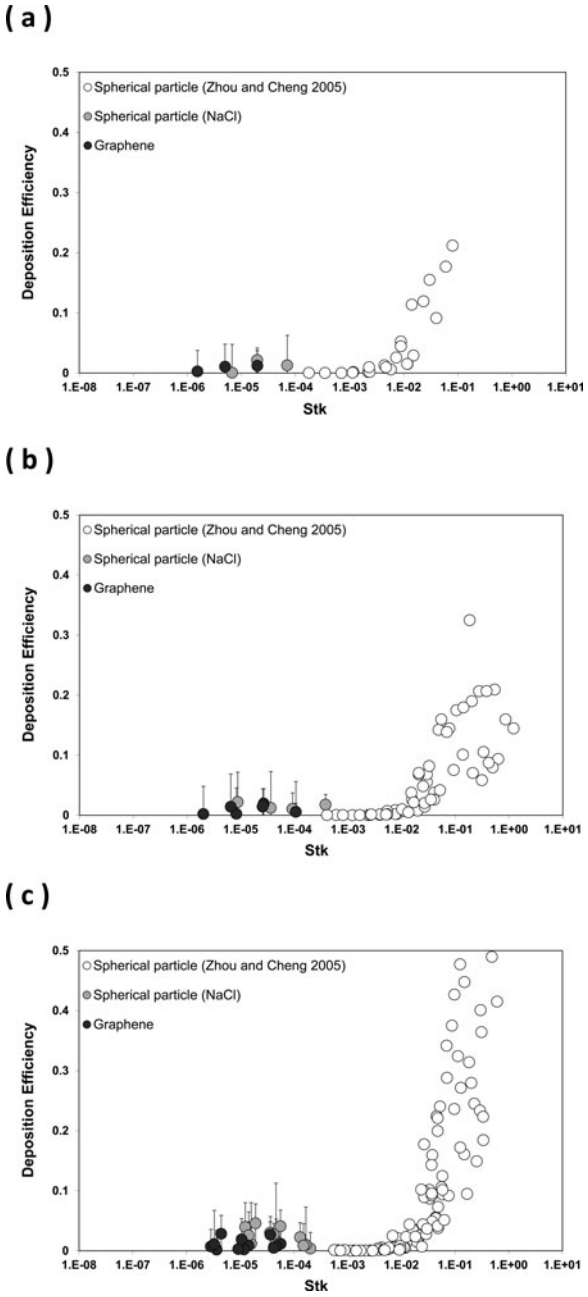

Figure 10. The deposition efficiency of graphene aerosols in the human tracheobronchial airways as a function of the Stokes number (a) 1st lung generation, (b) 2nd lung generation, and (c) 3rd lung generation.

on aggregate nanoparticles and nanofibers.[23,36] In those studies, ρ_{eff} was also found to decrease as the particle diameter increased. With these ρ_{eff} acquired, the d_{ae} for corresponding size classified graphene aerosols could be estimated. The calculated d_{ae} for 51, 101, 215 nm size classified graphene aerosols were 47, 84, 167 nm, respectively, as shown in Figure 6.

The graphene aerosol fractional deposition map shown in Figures 7 and 8 indicate that the deposition of graphene aerosols in human airway replicas was generally low and expressed basically no appreciable difference between different classification diameters. This result might be owing to the fact that the sizes of the graphene aerosols used in this study are all in the regime in which the airway depositions are not significantly affected by the size of the aerosols. As can be seen in Figures 7 and 8, the deposition fractions were less than 4% in general for all airway sections examined, and no apparent deposition pattern or trend was shown regarding the location of the airway section in the oral-to-lung airway replica. In the nasal airway, the graphene aerosol deposition fraction ranged from 1.3–2.4%. In the oral-to-lung airway, a considerable portion of the inhaled graphene aerosols were found to deposit in the oral airway (1.7–3.1%), and the deposition fractions in the tracheobronchial airways from the 2nd to the 4th lung generations were found generally less than 1%. The relatively high deposition fraction shown in the oral airway might be due to the fact that the oral airway (from the oral cavity to the larynx) contains a relatively larger total surface area for graphene aerosols to deposit. The total accumulated deposition fraction of the graphene aerosol in both nasal and oral-to-lung airways together was around 10% for all three classification diameters. These results indicate that nearly 90% of the graphene aerosols (with the diameter studied in this research) inhaled into the human airway could easily penetrate through to the human upper airways.

Figures 9 and 10 express that the deposition efficiency of the size classified graphene aerosols in the human airways were generally less than 0.03. Some published studies in literature reported similar deposition results as in this study, concluding that ultrafine particles with comparable diameters demonstrated a low airway deposition.[15,16] Here, the low airway deposition efficiencies shown in our study prove again that most of the graphene aerosols entering into the human respiratory tract can easily penetrate through airway sections in the upper airways. Also seen in Figures 9 and 10 is that, in comparing the deposition efficiencies of graphene aerosols to those of NaCl particles, the data points were scattered and showed no significant discrepancy between graphene aerosols and NaCl aerosols. This result implies that the size classified graphene and NaCl aerosols generated in this study possessed similar aerodynamic behaviors in the airway, which produced comparable airway deposition efficiencies. Moreover, it can be noticed that data points in Figures 9 and 10 seem to be able to connect smoothly between the nano-scale data group (solid data points) and the micro-scale data group (hollow data points on the right hand side), forming a smooth "S-like" data trend. This sigmoidal data trend reveals a well-recognized characteristic of aerosol airway deposition: aerosol airway deposition increases proportionally to the aerosol inertia

(for aerosol size around 100 nm and up). According to this, the deposition mechanism for those large micro-scale aerosols shown in Figures 9 and 10 should be inertia impaction, and for those small nano-scale aerosols such as graphene aerosols, the deposition mechanism should be Brownian diffusion.

Based on all deposition results acquired from this study shown above, it is reasonable to summarize that graphene aerosols with isometric shape and diameters in nano-scale show a low airway deposition in the human upper airways from the nasal and oral to the 4th lung generation airways. Nevertheless, it is believed that, with the same classification diameter (d_B), a possible platelet-like (high aspect ratio) graphene aerosol could possess a distinct d_{ae} compared to an isometric graphene aerosol, which might generate a significantly different airway deposition result. Further graphene airway deposition studies should focus on investigating this issue. However, for conducting airway deposition experiments using platelet-like graphene aerosols, a big challenge we must overcome first is to discover an optimal method to generate platelet-like graphene aerosols with concentrations high enough to sufficiently conduct size classification and the consequent airway deposition experiment.

Conclusion

Studying the deposition of graphene naomaterial aerosols in the human airway is very important from the viewpoint of occupational health since graphene materials inevitably could become airborne during the manufacturing process in the workplace. In this study, graphene aerosols were generated, size classified, and delivered into human upper airway replicas for airway deposition experiments using a novel experimental approach. The fractional deposition map obtained from this study showed that the graphene aerosol deposition in the airway sections studied were all less than 4%, and the deposition efficiency obtained in each airway section was generally lower than 0.03. This result implies that most of the graphene aerosols inhaled into the respiratory tract would enter the lower airways; therefore, worker exposure to graphene aerosols in related workplaces could result in a considerable amount of graphene aerosols entering the deep lung, where adverse health effects could possibly be induced. Also in this study, it was found that nano-scale aerosols having similar d_B will behave similarly in the airway, causing comparable deposition efficiencies in the airways. The experimental approach employed in this deposition study proved to be a desired experimental method for carrying out airway deposition studies using size classified aerosols.

Acknowledgments

The authors are grateful to Eileen Kuempel at NIOSH for developing the concept of this research project and to Bean T. Chen and Bahman Asgharian for useful suggestions on data analysis.

Funding

This project was sponsored by NIOSH contract 254-2010-M-36304, 214-2012-M-52048 and research grant R01OH010062.

References

[1] **Novoselov, K.S., A.K. Geim, S.V. Morozov, D. Jiang, Y. Zhang, S.V. Dubonos:** Electric field effect in atomically thin carbon films. *Science 306*:666–669 (2004).
[2] **Geim, K.:** Graphene: status and prospects. *Science 324*:1530–1534 (2009).
[3] **Seabra, A.B., A.J. Paula, R. Lima, O.L. Alves, and N. Duran:** Nanotoxicity of graphene and graphene oxide. *Chem. Res. Toxicol. 27*:159–168 (2014).
[4] **Kim, K.S., Y. Zhao, H. Jang, S.Y. Lee, J.M. Kim, K.S. Kim:** Large-scale pattern growth of graphene films for stretchable transparent electrodes. *Nature 457*:706–710 (2009).
[5] **De Volder, M.F.L., S.H. Tawfick, R.H. Baughman, and A.J. Hart:** Carbon nanotubes: present and future commercial applications. *Science 339*:535–539 (2013).
[6] **Jastrzebska M.A., P. Kurtycz, and A. R. Olszyna:** Recent advances in graphene family materials toxicity investigations. *J. Nanopart. Res.14*:1320 (2012).
[7] **Wang, K., J. Ruan, H. Song, J. Zhang, Y. Wo, S. Guo:** Biocompatibility of graphene oxide. *Nanoscale Res. Lett. 6*:8 (2011).
[8] **Zhang, X.Y., J.L. Yin, C. Peng, W.Q. Hu, Z.Y. Zhu, W.X. Li:** Distribution and biocompatibility studies of graphene oxide in mice after intravenous administration. *Carbon 49*(3):986–995 (2011).
[9] **Duch, M.C., G.R. Budinger, Y.T. Liang, S. Soberanes, D. Urich, S.E. Chiarella:** Minimizing oxidation and stable nanoscale dispersion improves the biocompatibility of graphene in the lung. *Nano Lett. 11*:5201–5207 (2011).
[10] **Schinwald A., F.A. Murphy, A. Jones, W. MacNee, and K. Donaldson:** Graphene-based nanoplatelets: a new risk to the respiratory system as a consequence of their unusual aerodynamic properties. *ACS Nano 6*(1):736–746 (2012).
[11] **Zhang, Y., S.F. Ali, E. Dervishi, Y. Xu, Z. Li, D. Casciano, and A.S. Biris:** Cytotoxicity effects of graphene and single-wall carbon nanotubes in neural phaeochromocytoma-derived PC12 cells. *ACS Nano 4*(6):3181–3186 (2010).
[12] **Vallabani, N.V.S., S. Mittal1, R.K. Shukla, A.K. Pandey, S.R. Dhakate, R. Pasricha:** Toxicity of Graphene in Normal Human Lung Cells (BEAS-2B). *J. Biomed. Nanotechnol.7*:106–107 (2011).
[13] **Hu, W., C. Peng, M. Lv, X. Li, Y. Zhang, N. Chen:** Protein corona-mediated mitigation of cytotoxicity of graphene oxide. *ACS Nano 5*(5):3693–3700 (2011).
[14] **Heitbrink, W.A., L.M. Lo, and K.H. Dunn:** Exposure controls for nanomaterials at three manufacturing sites. *J. Occup. Environ. Hyg. 12*(1):16–28 (2015).

[15] **Cohen, B.S., R.G. Sussman, and M. Lippmann:** Ultrafine particle deposition in a human tracheobronchial cast. *Aerosol Sci. Technol. 12*:1082–1091 (1990).
[16] **Smith, S., Y.S. Cheng, and H.C. Yeh:** Deposition of ultrafine particle in human tracheobronchial airway of adults and children. *Aerosol Sci. Technol. 35*:697–709 (2001).
[17] **Zhou, Y., and Y.C. Cheng:** Particle deposition in a cast of human tracheobronchial airways. *Aerosol Sci. Technol. 39*:492–500 (2005).
[18] **Su, W.C., and Y.S. Cheng:** Carbon nanotubes size classification, characterization, and nasal airway deposition. *Inhal. Toxicol. 26*(14):843–852 (2014).
[19] **Su, W.C., and Y.S. Cheng:** Estimation of carbon nanotubes deposition in a human respiratory tract replica. *J. Aerosol Sci. 79*:72–85 (2015).
[20] **Johnsson, A.C., M.C. Camerani, and Z. Abbas:** Combined electrospray-SMPS and SR-SAXS investigation of colloidal silica aggregation. part I. influence of starting material on gel morphology. *J. Phys. Chem. B 115*(5):765–775 (2011).
[21] **Ku, B.K., and P. Kulkarni:** Morphology of single-wall carbon nanotube aggregates generated by electrospray of aqueous suspensions. *J. Nanoparticle Res. 11*(6):1393–1403 (2009).
[22] **McMurry, P.H., X. Wang, K. Park, and K. Ehara:** The relationship between mass and mobility for atmospheric particles: a new technique for measuring particle density. *J. Aerosol Sci. 36*:227–238 (2002).
[23] **Park, K., F. Cao, D.B. Kittelson, and P.H. McMurry:** Relationship between particle mass and mobility for diesel exhaust particles. *Environ. Sci. Technol. 37*:577–583 (2003).
[24] **Subramaniam, R.P., R.B. Richardson, K.T. Morgan, J.S. Kimbell, and R.A. Guilmette:** Computational fluid dynamics simulations of inspiratory airflow in the human nose and nasopharynx. *Inhal. Toxicol. 10*:91–120 (1998).
[25] **Zwartz, G.J., and R.A. Guilmette:** Effect of flow rate on particle deposition in a replica of a human nasal airway. *Inhal. Toxicol.13*:109–127 (2001).
[26] **Cheng, Y.S., T.D. Holmes, J. Gao, et al.:** Characterization of nasal spray pumps and deposition pattern in a replica of human nasal airway. *J. Aerosol Med. 14*(2):267–280 (2001).
[27] **Su, W.C., J. Wu, and Y.S. Cheng:** Deposition of man-made fiber in a human nasal airway. *Aerosol Sci. Technol. 42*:173–181 (2008).
[28] **Cheng, Y.S., S.M. Smith, and H.C. Yeh:** Deposition of ultrafine particles in human tracheobronchial airways. *Ann. Occup. Hyg. 41*(S1):714–718 (1997).
[29] **Zhou, Y., W.C. Su, and Y.S. Cheng:** Fiber deposition in the tracheobronchial region: Deposition equations. *Inhal. Toxicol. 20*(13):1191–1198 (2008).
[30] **Cheng, Y.S., Y. Zhou, and B.T. Chen:** Particle deposition in a cast of human oral airways. *Aerosol Sci. Technol. 31*:286–300 (1999).
[31] **Su, W.C., and Y.S. Cheng:** Deposition of man-made fibers in human respiratory airway casts. *J. Aerosol Sci. 40*(3):270–284 (2009)
[32] **NCRP:** National council on radiation protection and measurement: deposition, retention and dosimetry of inhaled radioactive substances, NCRP Report No. 125, National Council on Radiation Protection and Measurement, Bethesda, MD (1997).
[33] **Su, W.C., and Y.S. Cheng:** Fiber deposition pattern in two human respiratory tract replicas. *Inhal. Toxicol. 18*:749–760 (2006).
[34] **Cheng, K.H., Y.S. Cheng, H.S. Yeh, and D.L. Swift:** Deposition of ultrafine aerosols in the head airways during natural breathing and during simulated breath holding using replicate human upper airway casts. *Aerosol Sci. Technol. 23*:465–474 (1995).
[35] **Kelly, J.T., B. Asphgrian, J.S. Kimbell, and B.A. Wong:** Particle deposition in human nasal airway replicas manufactured by different methods. Part II: Ultrafine particles. *Aerosol Sci. Technol. 38*:1072–1079 (2004).
[36] **Ku, B.K., M.S. Emery, A.D. Maynard, M.R. Stolzenburg, and P.H. McMurry:** In situ structure characterization of airborne carbon nanofibers by a tandem mobility-mass analysis. *Nanotechnology 16*:3613–3621 (2006).